Neurobiology of Aging 36 (2015) 971–981

Contents lists available at ScienceDirect

Neurobiology of Aging

journal homepage: www.elsevier.com/locate/neuaging

Axonal transport declines with age in two distinct phases separated by a period of relative stability☆

Stefan Milde [1], Robert Adalbert [1], M. Handan Elaman, Michael P. Coleman*

Signalling ISP, The Babraham Institute, Babraham Research Campus, Cambridge, UK

ARTICLE INFO

Article history:
Received 12 June 2014
Received in revised form 12 September 2014
Accepted 17 September 2014
Available online 28 September 2014

Keywords:
Axonal transport
Aging
Nicotinamide mononucleotide
Adenylyltransferase 2
Mitochondrial transport
Axon regeneration
Fluorescence live imaging

ABSTRACT

Axonal transport is critical for supplying newly synthesized proteins, organelles, mRNAs, and other cargoes from neuronal cell bodies into axons. Its impairment in many neurodegenerative conditions appears likely to contribute to pathogenesis. Axonal transport also declines during normal aging, but little is known about the timing of these changes, or about the effect of aging on specific cargoes in individual axons. This is important for understanding mechanisms of age-related axon loss and age-related axonal disorders. Here we use fluorescence live imaging of peripheral nerve and central nervous system tissue explants to investigate vesicular and mitochondrial axonal transport. Interestingly, we identify 2 distinct periods of change, 1 period during young adulthood and the other in old age, separated by a relatively stable plateau during most of adult life. We also find that after tibial nerve regeneration, even in old animals, neurons are able to support higher transport rates of each cargo for a prolonged period. Thus, the age-related decline in axonal transport is not an inevitable consequence of either aging neurons or an aging systemic milieu.

1. Introduction

The unique architecture of axons poses a significant demand on the cell body, as most newly synthesized proteins, organelles, and mRNAs originate in the soma and require long-distance delivery into axons. Axonal dysfunction and impaired axonal transport are frequently described as among the earliest and possibly causative changes in age-related neurodegenerative diseases (Adalbert and Coleman, 2013; Millecamps and Julien, 2013).

As axonal transport declines during normal aging, this could combine with disease-associated impairments to accelerate pathology. However, little is known about the nature of this decline in individual axons, specifically regarding timing, affected cargoes, similarities between peripheral nerves and the central nervous system (CNS), and the potential to reverse these changes. Most studies either analyze the bulk transport of several cargoes in all axons of a nerve (Brunetti et al., 1987; Cross et al., 2008; Frolkis et al., 1997; Geinisman et al., 1977; McQuarrie et al., 1989; Stromska and Ochs, 1982) or investigate a specific cargo in all axons (Castel et al., 1994; Fernandez and Hodges-Savola, 1994; Goemaere-Vanneste et al., 1988; Li et al., 2003; McMartin and O'Conner, 1979; Tashiro and Komiya, 1994) without giving insight into individual axons. It is, for example, important to clarify whether a global reduction in axonal transport reflects reduced transport in individual axons or simply axon loss. Conventional tracking of radiolabeled cargoes or newer approaches using tetanus neurotoxin (Millecamps and Julien, 2013) do not easily allow this distinction. Video-enhanced imaging provides information on transport rates in individual axons (Viancour and Kreiter, 1993) but does not easily distinguish between different cargoes. Mitochondrial transport declines in individual peripheral nerve axons between 8 and 24 months of age (Gilley et al., 2012), but how much this is representative of other cargoes and other regions of the nervous system, especially in the CNS, remains unknown. In addition, little is known about when during adulthood these changes occur, or whether they can be reversed.

Live-imaging studies of axonal transport in nervous system tissue have largely focused on mitochondria (Gilley et al., 2012; Mar et al., 2014; Marinkovic et al., 2012; Misgeld et al., 2007) but whether this is fully representative of other cargoes is unclear. One cargo that appears to be of particular importance is nicotinamide mononucleotide adenylyltransferase 2 (NMNAT2), as we propose that a reduced supply of this critical axon-survival factor could place axons at increased risk of degeneration (Conforti et al., 2014). We previously described the use of NMNAT2-Venus mice to visualize axonal transport of fluorescently tagged NMNAT2 (Milde et al., 2013a). Here,

* Corresponding author at: The Babraham Institute, B540, Babraham Research Campus, Babraham, Cambridge, CB22 3AT, UK. Tel.: 0044 (0)1223 496315; fax: 0044 (0) 1223 496348.
E-mail address: michael.coleman@babraham.ac.uk (M.P. Coleman).

[1] S.M. and R.A. contributed equally to this work.

0197-4580/$ – see front matter
http://dx.doi.org/10.1016/j.neurobiolaging.2014.09.018

we use live imaging of peripheral nerve and CNS explants to study age-associated changes in the fast axonal transport of NMNAT2 and mitochondria. The data reveal 2 separate periods of declining axonal transport in some parts of the nervous system, 1 period as the growth phase plateaus and the other in old age. Intriguingly, we show that neurons in aged mice are still capable of supporting higher rates of fast axonal transport, suggesting the existence of signals that can reverse the age-related decline in axonal transport.

2. Methods

2.1. Animals

All animal work was approved by the Babraham Institute Animal Welfare and Experimentation Committee and carried out in accordance with the Animals (Scientific Procedures) Act, 1986, under Project Licenses 80/2254 and 70/7620. The generation, breeding, genotyping, and initial characterization of NMNAT2-Venus mice expressing NMNAT2-YFP(Venus) under the neuron-specific Thy1.2 promoter was described previously (Milde et al., 2013a). MitoS mice (Thy1.2-MitoCFP-S) (Misgeld et al., 2007) were kindly provided by Prof. Martin Kerschensteiner (University Munich) and Prof. Thomas Misgeld (TU Munich). Animals were used for transport imaging (see 2.3 below) at indicated ages (see Results). Sample sizes for all age groups are shown in Table 1. We observed no significant difference between transport parameters in male and female animals of the same age for any of the measures used, so data from both sexes was combined for all analyses. All animals were heterozygous for the relevant transgene and C57BL/6JBabr mice (Babraham Institute) were used for breeding. Animals were kept on a 12:12 hours light:dark cycle at a constant temperature of 19 °C in a pathogen-free environment with up to 5 animals per cage.

2.2. Preparation of acute PNS and CNS tissue explants

Mice were humanely killed by cervical dislocation followed by exsanguination. For analysis of PNS axonal transport, sciatic nerves were dissected rapidly and immersed immediately into pre-warmed (37 °C), pre-oxygenated Neurobasal-A medium (Gibco). For analysis of CNS axonal transport, mice were subsequently decapitated and the head immersed in pre-warmed, pre-oxygenated Neurobasal-A medium. Optic nerves and the fimbria of the hippocampus were then dissected out and transferred into pre-warmed oxygenated Neurobasal-A medium. Optic nerves were removed by transection behind the eye globe and at the rostral limit of the optic chiasm. To remove the fimbria of hippocampus, first the cortex and striatum were dissected out on both sides of the brain, followed by the hippocampus. The fimbria and body of fornix were cleaned of any attached gray matter before imaging. Axonal transport recordings were performed on the ventral side of the fimbria.

Table 1
Sample sizes for axonal transport study

Genotype	Age (mo)	Total animals in group	Analyzed sciatic nerve	Analyzed optic nerve	Analyzed fimbria
NMNAT2-Venus	1.5	10	9	10	10
	3	27	25	27	18
	6	10	9	10	5
	12	8	7	8	7
	18	10	9	9	9
	24	10	10	8	10
MitoS	3	9	9	N/A	N/A
	6	6	6	N/A	N/A
	12	6	6	N/A	N/A

Group sizes for animals of different genotypes and ages used for live imaging of axonal transport. In some cases, animals had to be excluded from the analysis for a specific tissue because of damage to the tissue during the dissection process. "Analyzed" refers to the number of animals included in the statistical analysis for each tissue and age group.
Key: N/A, not applicable.

2.3. Live imaging of axonal transport

Imaging of axonal transport in tissue explants was performed on an Olympus Cell imaging system (IX81 microscope, Hamamatsu ORCA ER camera, ×100 1.45 NA apochromat objective). During imaging, tissues were maintained in oxygenated Neurobasal-A medium at 37 °C in an environment chamber (Solent Scientific). Images were captured using fixed light intensity and camera exposure time settings at a rate of 2 frames per second for 1.5 to 3 minutes. Five to 10 individual movies (often containing multiple axons) were captured for each tissue explant. To ensure reproducibility between experimental days, 3-month-old animals were imaged on all experimental days along with animals of other ages. The order of imaging was varied randomly between animals of different ages.

2.4. Image processing and quantification

Individual axons were straightened (except where indicated) using the Straighten plugin in ImageJ software version 1.44 (Rasband, W.S., ImageJ, U. S. National Institutes of Health, Bethesda, MD; http://imagej.nih.gov/ij/, 1997–2012). Axonal transport parameters were determined for individual axons using the DifferenceTracker set of ImageJ plugins (Andrews et al., 2010). The principal output of these plugins is the number of moving particles identified in each frame of the image, normalized to axon length (presented as particle count per second per 100 μm axon length) and the average and maximum velocities of the detected moving particles (shown in μm/s). It is important to note that the plugin does not track a particle once it has become stationary and thus does not take into account pauses in movement or reversals of direction. These are instead represented as new tracks in the output (see Andrews et al., 2010). Details of analysis parameters are listed in Table 2. On average, 14, 12, and 17 axons were analyzed for each sciatic nerve, optic nerve and fimbria explant, respectively.

2.5. Nerve crush and regeneration

For nerve crush and regeneration experiments, MitoS (n = 4, male) and NMNAT2-Venus (n = 4, female) animals at 23 months of age were anaesthetized with isoflurane and the distal part of the sciatic nerve was exposed and crushed above knee level by applying firm pressure using fine forceps (Dumont #5) for 20 seconds. The wound was closed using tissue adhesive and animals were allowed to recover. Four weeks after surgery, recovery of motor function was assessed based on gait, grasp and posture, all of which showed good functionality. Eight weeks after surgery, animals were killed by cervical dislocation, and both tibial nerves were dissected and processed for live imaging as described above. Both tibial nerves were removed into warm, oxygenated Neurobasal A medium immediately after the animal had been killed. The order of imaging of control and crushed nerves was alternated between animals to control for the amount of time that nerves were kept in medium before imaging. After live imaging, nerves were processed for semi-thin sectioning (500-nm section thickness), staining, and imaging as described previously (Adalbert et al., 2005; Milde et al., 2013a), to confirm the extent of axon regeneration and to assess the morphology of the regenerated nerve.

Table 2
Imaging and analysis parameters

Genotype	Tissue	Acquisition rate (frames/s)	Total duration (frames)	Axon width for straightening (pixels)	Contrast adjustment (% saturated)	Difference filter		Despeckle	Mass particle tracker			
						Minimum difference	Difference frame offset		Minimum tracked intensity	Minimum feature size	Initial flexibility	Subsequent flexibility	Minimum track length
NMNAT2-Venus (NMNAT2-YFP) line 8	Sciatic nerve	2	240	30	1	40	4	No	20	2	15	10	4
	Optic nerve	2	120	21	5	30	4	Yes	20	2	15	10	4
	Fimbria	2	120	21	5	20	4	Yes	20	2	15	10	4
MitoS (mito-CFP)	Sciatic nerve	2	360	30	5	10	4	Yes	20	2	8	5	4

Parameters used for live imaging of axonal transport of mitochondria (MitoS) and NMNAT2 (NMNAT2-Venus) in various tissue explants, and settings used for analysis of axonal transport using ImageJ plugins (Straighten, Enhance Contrast, Difference Filter, Despeckle, Mass Particle Tracker).

2.6. Statistical analysis

Statistical analyses were performed using GraphPad Prism 6 (GraphPad Software Inc) and SPSS Statistics 20 (IBM). Where indicated, age groups were combined to increase statistical power.

3. Results

The critical axon survival factor NMNAT2 (Gilley and Coleman, 2010; Gilley et al., 2013) associates with a Golgi-derived axonal transport vesicle population through palmitoylation of a double-cysteine motif in its central isoform-specific targeting and interaction domain (Lau et al., 2010; Milde et al., 2013b) and undergoes fast axonal transport (Gilley and Coleman, 2010; Milde et al., 2013a). To study the transport parameters of NMNAT2 vesicles in aging animals, we used NMNAT2-Venus mice (Milde et al., 2013a). We assayed axonal transport using fluorescence live imaging of acute tissue explants combined with semi-automated image analysis using the ImageJ DifferenceTracker plugins with settings shown in Table 2 (see Methods). (Andrews et al., 2010). This method allows an unbiased quantification of the number and velocities of moving particles. Importantly, however, stationary or pausing particles are excluded from the analysis and not quantified (see Methods for details). For a thorough characterization of the time course of age-associated changes, we studied 6 groups of animals at ages ranging from 1.5 to 24 months.

3.1. Age-associated changes in NMNAT2-Venus transport in peripheral nerve

To investigate age-associated changes of NMNAT2 vesicles in peripheral axons, we imaged and quantified the axonal transport of NMNAT2-Venus particles in sciatic nerve axons (Fig 1A). Average (total displacement of a particle/time tracked) and maximal (farthest displacement of each tracked particle between 2 frames) particle velocities in both anterograde and retrograde directions remained stable from 1.5 and 18 months, but then reduced significantly in animals at 24 months of age (Fig 1B and C). Surprisingly, the number of particles observed moving anterogradely and retrogradely showed a significant drop even in young animals between the ages of 3 and 6 months. This was followed by a relatively stable plateau that was maintained at least up to 18 months. From 18 to 24 months, another significant reduction in the number of anterogradely moving particles was observed, along with a similar, but statistically nonsignificant trend in the retrograde direction (Fig 1D and E). To test whether these changes could have been caused by changes in expression level of the transgene over the lifetime of the animals, which might impair tracking of particles, we quantified the average fluorescence intensity of labeled axons from animals of different ages. As shown in Table 3, there were no consistent trends or differences in fluorescence intensity that would explain the observed changes in the number of moving particles.

The significant drop in transport rates of NMNAT2-Venus particles observed from 3 to 6 months of age prompted us to ask whether this was a general effect on multiple fast axonal transport cargoes, or perhaps a more specific effect on NMNAT2 vesicles. To start addressing this question, we imaged mitochondrial transport in sciatic nerves of MitoS mice expressing mitochondrially targeted CFP under the same Thy1.2 promoter (Fig 2A). We previously reported a fall in axonal transport in these mice between 8 and 24 months (Gilley et al., 2012), but earlier ages have not been studied. Here, we observed a significant drop in the number of anterogradely and retrogradely transported mitochondria from 3 to 6 months of age, with no further change until at least 12 months (Fig 2B and C). Over the same time course, no significant changes in transport velocities were observed (Fig 2D and E). As for

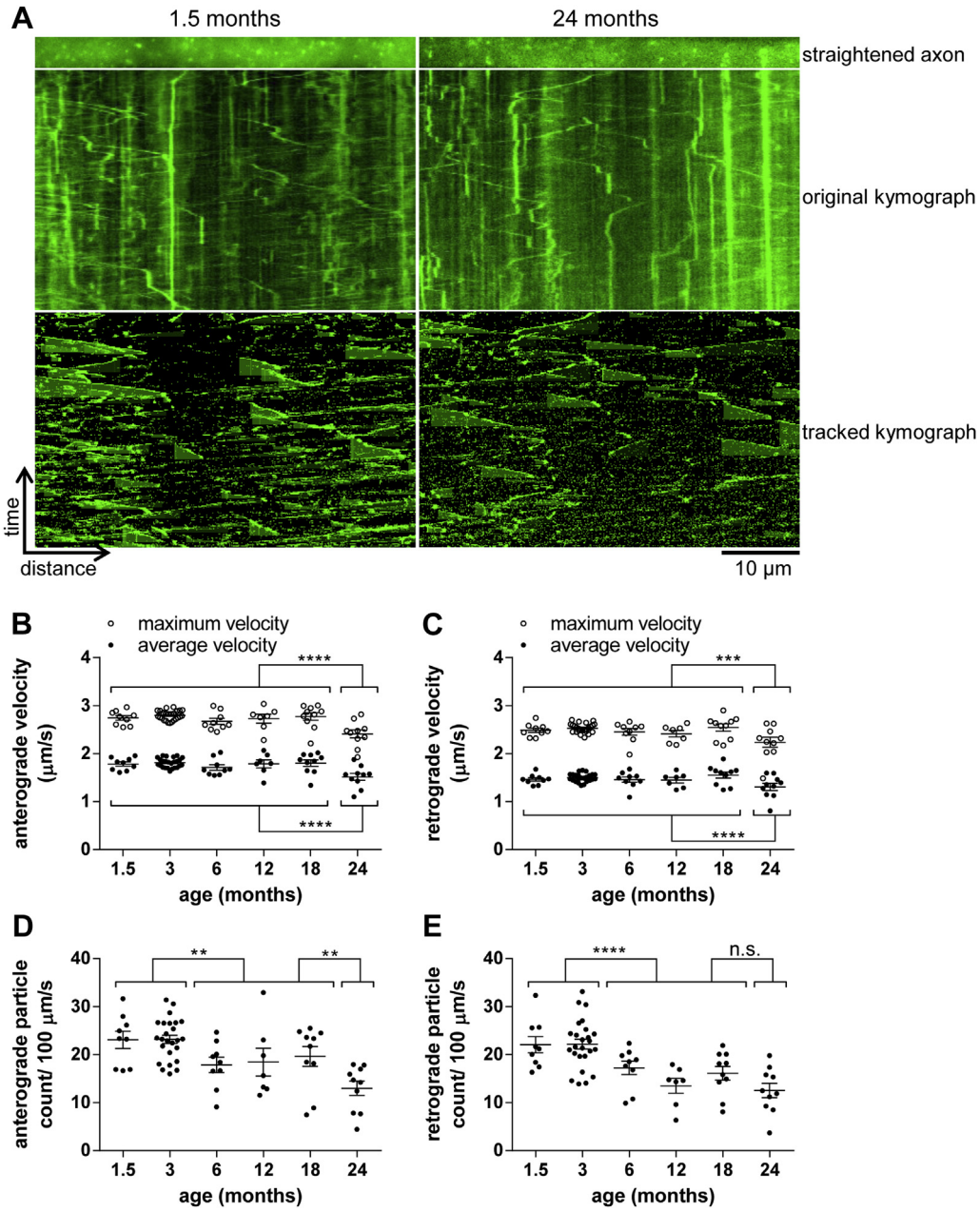

Fig. 1. Age-associated changes in NMNAT2-Venus axonal transport in sciatic nerve axons. (A) Representative straightened axon, kymograph, and kymograph of tracked particles of NMNAT2-Venus transport in sciatic nerves of 1.5- and 24-month-old NMNAT2-Venus (line 8) mice. The straightened axon represents the first frame of the time lapse recording (total 240 frames; frame rate 2 fps) that was used to generate the original kymograph. Moving particles were tracked using the ImageJ Difference Tracker set of plugins (see Table 2 for analysis parameters) and another kymograph generated to show successfully tracked particles. (B–E) Quantification of axonal transport parameters in sciatic nerve explants from NMNAT2-Venus line 8 animals of indicated ages. For all graphs, each data point represents the mean value obtained for 1 animal (5 fields of view and, on average, 14 axons per animal). Horizontal bar indicates mean, error bars are SEM. *Statistically significant difference between indicated ages or groups of ages. ($^{*}p < 0.05$, $^{**}p < 0.01$, $^{***}p < 0.001$, $^{***}p < 0.0001$; 1-way analysis of variance with Tukey multiple comparisons post-test or Student *t* test). The following parameters are shown: (B) anterograde particle velocity, (C) retrograde particle velocity, (D) anterograde particle count, and (E) retrograde particle count. (For interpretation of the references to color in this Figure, the reader is referred to the web version of this article.)

NMNAT2-Venus above, changes in the average fluorescence intensity of labeled axons are unlikely to account for these differences (Table 3). These findings parallel the results for NMNAT2-Venus above and suggest a general reduction in fast axonal transport rates in peripheral nerves between 3 and 6 months of age, followed by a more stable plateau during adult life. Combined with our findings in older MitoS mice (Gilley et al., 2012), these results suggest 2 major periods of reduction in the fast axonal transport of several cargoes, 1 occurring in young animals between 3 and 6 months of age, and the other during old age after 18 months.

3.2. Age-associated changes in NMNAT2-Venus transport in optic nerve

Most of the existing studies that have reported fluorescence live imaging of axonal transport have, presumably at least in part because of technical difficulties, focused on the peripheral nervous system. However, many age-associated neurodegenerative conditions affect the CNS (Adalbert and Coleman, 2013; Millecamps and Julien, 2013), highlighting the need to understand how aging affects the function of CNS neurons, including their axonal transport. Thus,

Table 3
Average fluorescence intensity of labeled axons at selected ages

Genotype	Age (mo)	Average fluorescence intensity of labeled axons (arbitrary units mean ± SEM)		
		Sciatic nerve	Optic nerve	Fimbria
NMNAT2-Venus	1.5	522 ± 33	127 ± 17	346 ± 15
	6	545 ± 22	221 ± 45	329 ± 14
	18	495 ± 22	315 ± 19	318 ± 18
	24	540 ± 27	204 ± 17	302 ± 16
MitoS	3	523 ±32	N/A	N/A
	6	538± 32	N/A	N/A

Key: N/A, not applicable; SEM, standard error of the mean.

we aimed to use NMNAT2-Venus mice to investigate age-associated changes in CNS axonal transport. The first tissue that we studied in this way was the optic nerve. In addition to technical advantages (easy accessibility, rapid dissection), degeneration of retinal ganglion cells and their axons, which constitute the optic nerve, contributes critically to pathology in glaucoma (Beirowski et al., 2008; Chidlow et al., 2011; Howell et al., 2007). Bidirectional fast axonal transport of NMNAT2-Venus particles was readily and reproducibly detectable in optic nerve explants. Individual axons were identified in time-lapse recordings and straightened, and quantification of axonal transport was performed in the same way as for sciatic nerve axons, above (Fig 3A). However, the dissection and imaging procedures used here mean that anterograde and retrograde transport were not analyzed separately and, instead, only overall transport rates were measured. Interestingly, we observed an overall similar profile of transport changes from 1.5 to 24 months of age as for sciatic nerve axons. However, the reduction in the number of moving particles at a young age occurred earlier, from 1.5 to 3 months, with a stable plateau from 3 to 18 months and a further significant drop at 24 months of age (Fig 3B). Average and maximal transport velocities were more variable overall than for sciatic nerve, but no consistent trends or significant changes were observed (Fig 3C). Although the average fluorescence intensity of labeled axons in the optic nerve varied somewhat with age (Table 3), there is no decline relative to young mice and no consistent relationship between increases or decreases in label intensity and the number of moving particles detected. Thus, simple changes in expression level are unlikely to account for the observed differences. Instead, these results indicate that, as for sciatic nerve axons above, 2 phases of reductions in axonal transport rates in young and old animals are separated by a stable plateau in adults.

3.3. Age-associated changes in NMNAT2-Venus transport in fimbria

To extend our observations to an additional CNS region, we chose the fimbria of the hippocampus. This white matter bundle consists of a large number of parallel axons that can be dissected free from surrounding tissue while maintaining a considerable length of intact axon. Although some optimization of dissection technique and duration was required (Fig 4A–H and Methods), we reproducibly observed a large number of bidirectionally mobile particles undergoing fast axonal transport along the axon tracts in the left and right side fimbria. Individual axon tracts were straightened and axonal transport was quantified as described above. It is important to note that the bidirectional orientation of axons in this area prevents separate analysis of anterograde and retrograde axonal transport (Fig 4I). As in optic and sciatic nerves, axonal transport of NMNAT2-Venus in the fimbria decreased significantly during the first few months of life. We observed a significant drop in the number of NMNAT2-Venus particles undergoing axonal transport from 1.5 to 3 and from 3 to 6 months of age, followed by a stable plateau (Fig 4J). Intriguingly, there was no evidence of a second period of decreasing axonal transport rates up to 24 months of age. Instead, the plateau observed in adult animals from 6 months onward appeared to be stable until at least 24 months. Over the complete time course of our analysis, no significant changes in average or maximal transport velocities were observed (Fig 4K). These findings hint at possible tissue-specific effects of old age on axonal transport rates of NMNAT2-Venus particles. As for the other tissues investigated, changes in the average fluorescence intensity of labeled axons are unlikely to account for the observed differences in transport (Table 3). We also attempted to measure mitochondrial transport in optic nerve and fimbria explants from MitoS mice in the same way as for NMNAT2-Venus. However, a reliable quantification of mitochondrial transport in these tissues was not achieved, as we frequently observed little or no movement with mitochondria that had adopted a rounded-up morphology (data not shown). This could be linked to the known sensitivity of mitochondrial trafficking to calcium influx (Wang and Schwarz, 2009) and suggests that, for analysis of CNS axonal transport in explanted tissue, NMNAT2-Venus mice could be a more robust model than MitoS.

3.4. Partial reversibility of age-associated decrease in axonal transport rates in peripheral nerves

Given the above results showing a significant decline in NMNAT2-Venus transport from 18 to 24 months of age in several parts of the nervous system, together with previous results indicating a similar decline in mitochondrial transport (Gilley et al., 2012), the possibility of reversing this decline could be useful both to study its consequences and for application in age-related disorders. To test whether aged neurons in an old systemic environment can, in principle, support a higher rate of transport given the right signals, we reasoned that a regenerative response could be a way to provide these signals. For this, we performed a crush injury in 1 of the tibial nerves in 23-month-old NMNAT2-Venus or MitoS mice. Peripheral nerve regeneration has been previously been shown to still occur in aged mice, albeit at slower speeds than in young mice (Tanaka and Webster, 1991; Tanaka et al., 1992), and in younger animals it is known to transiently enhance axonal transport (Mar et al., 2014; Misgeld et al., 2007). In agreement with this, we found that functional recovery was well advanced 4 weeks after injury, as judged based on posture, gait, and grasp. In order to focus the study on longer-term effects of nerve repair rather than any residual, longitudinal axon growth, we allowed animals to survive for several more weeks to study rates of axonal transport in the regenerated nerves at or approaching 8 weeks after the original injury. Semi-thin sections of tibial nerves from the injured leg revealed large numbers of intact myelinated axons, confirming that successful regeneration had taken place, with myelin sheaths and axon calibers still slightly thinner than in uninjured contralateral nerves as expected (Fig 5A). Interestingly, these regenerated axons also showed myelin irregularities similar to those observed in the uninjured control axons, suggesting that newly regenerated and remyelinated axons very quickly acquire these structural abnormalities in old animals.

Measuring the rates of axonal transport in these axons, we observed a consistent, statistically significant increase in the number of anterogradely moving particles in the regenerated axons in MitoS (Fig 5B) and NMNAT2-Venus mice (Fig 5D) compared to axons in the contralateral uninjured nerve. The regenerated nerves supported a level of anterograde axonal transport not dissimilar to those in much younger mice (Figs 1 and 2). Retrograde transport was not significantly increased in either MitoS (Fig 5C) or NMNAT2-Venus mice (Fig 5E), although we did observe a statistically nonsignificant trend for increased

retrograde transport in regenerated MitoS axons (Fig 5C). Average or maximum transport velocities were not altered in regenerated axons relative to uninjured control axons (data not shown). These findings suggest that neurons in 24- to 25-month-old mice are still capable of supporting significantly higher levels of axonal transport, indicating that the age-related decline in transport rates described above is at least partially reversible. Interestingly, the structural abnormalities and myelin invaginations we observed in the regenerated axons of MitoS and NMNAT2-Venus mice (Fig 5A), suggest that an improvement in the structural appearance of the regenerated axons is not required for this response.

4. Discussion

Here we report evidence to suggest that 2 independently transported cargoes—mitochondria and the axon survival factor NMNAT2—show a similar pattern of declining axonal transport during aging. An early drop between 1.5 and 6 months of age is followed by a stable plateau during adult life and a significant,

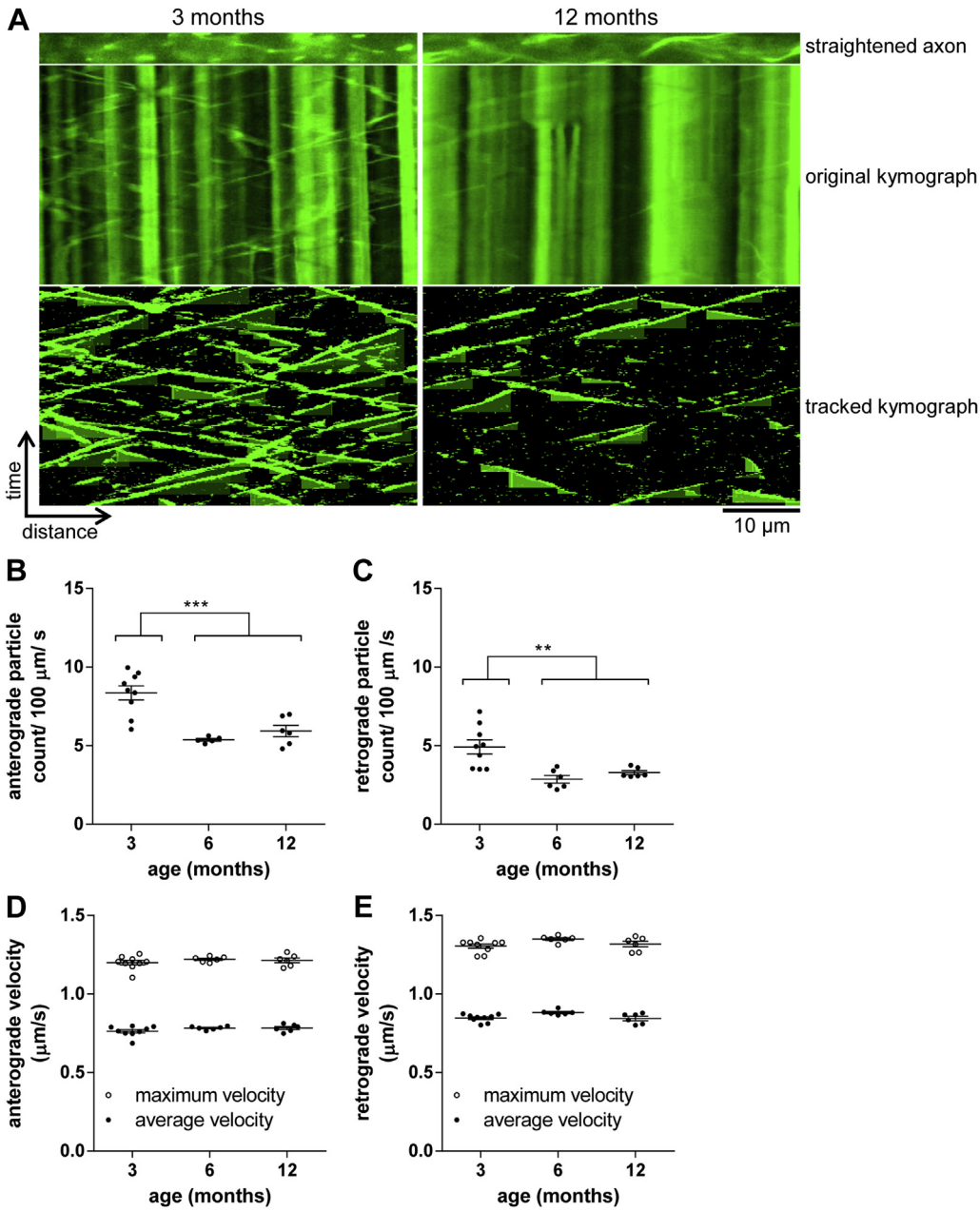

Fig. 2. Age-associated changes in mitochondrial transport in sciatic nerve axons. (A) Representative straightened axon, kymograph, and kymograph of tracked particles of mitochondrial transport in sciatic nerves of 3- and 12-month-old MitoS mice. The straightened axon represents the first frame of the time lapse recording (total 360 frames; frame rate 2 fps) that was used to generate the original kymograph. Moving particles were tracked using the ImageJ Difference Tracker set of plugins (see Table 2 for analysis parameters) and another kymograph generated to show successfully tracked particles. (B–E) Quantification of axonal transport parameters in sciatic nerve explants from MitoS animals of indicated ages. For all graphs, each data point represents the mean value obtained for 1 animal (5 fields of view and, on average, 19 axons per animal). Horizontal bar indicates mean and error bars standard error of the mean. Statistically significant differences between ages or groups of ages are indicated as follows: ** $p < 0.01$; ***$p < 0.001$ (Student t test). The following parameters are shown: (B) anterograde particle count, (C) retrograde particle count, (D) anterograde particle velocity, and (E) retrograde particle velocity. (For interpretation of the references to color in this Figure, the reader is referred to the web version of this article.)

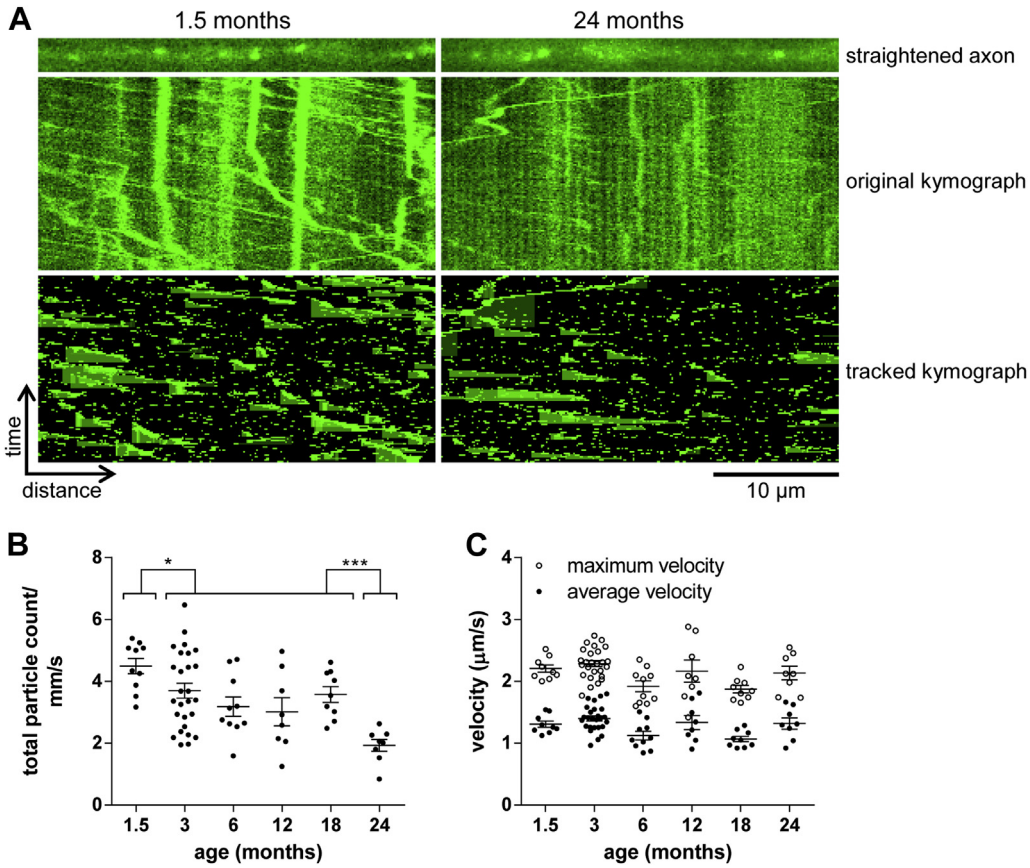

Fig. 3. Age-associated changes in NMNAT2-Venus axonal transport in optic nerve. (A) Representative straightened axon, kymograph, and kymograph of tracked particles of NMNAT2-Venus transport in optic nerve of 1.5- and 24-month-old NMNAT2-Venus (line 8) mice. The straightened axon represents the first frame of the time lapse recording (total 120 frames; frame rate 2 fps) that was used to generate the original kymograph. Moving particles were tracked using the ImageJ Difference Tracker set of plugins (see Table 2 for analysis parameters) and another kymograph generated to show successfully tracked particles. (B, C) Quantification of axonal transport parameters in optic nerve explants from NMNAT2-Venus line 8 animals of indicated ages. Each data point represents the mean value obtained for 1 animal (7 fields of view and, on average, 12 axons per animal). Horizontal bar indicates mean and error bars standard error of the mean. *Statistically significant difference between indicated ages or groups of ages. (*$p < 0.05$, *** $p < 0.001$; 1-way analysis of variance with Tukey multiple comparisons post-test). The following parameters are shown: (B) total particle count, (C) particle velocity. (For interpretation of the references to color in this Figure, the reader is referred to the web version of this article.)

tissue-specific reduction in transport rates after 18 months. Importantly, we find that such age-associated changes could be reversible, and that old neurons are still able to support higher rates of transport, similar to those observed in younger animals.

There are few existing studies of transport rates of a specific cargo in individual axons of aging animals, but we previously observed a significant decline in the rate of mitochondrial transport in MitoS mice from 8 to 24 months of age (Gilley et al., 2012). Although this study starts to shed light on the behavior of an individual organelle, the repertoire of cargoes studied needs to be extended for several reasons. First, mitochondria are most likely not representative for the majority of axonal transport cargoes. Vesicle-mediated and mitochondrial transport use different (albeit partially overlapping) sets of transport motors and adaptors (Hirokawa and Noda, 2008; Hirokawa et al., 2009), and we have shown that NMNAT2 and mitochondria are transported independently of one another in primary culture and in vivo (Milde et al., 2013a, 2013b). This means that impairments in the transport of 1 of these cargoes do not necessarily affect the other. Second, any alteration in the balance between mitochondrial fusion and fission in the axon could affect the perceived rates of mitochondrial axonal transport, especially because smaller mitochondria appear to move more frequently than larger ones (Misgeld et al., 2007). However, such processes would not necessarily affect vesicular axonal transport in the same way. Third, even the energy sources driving vesicular and mitochondrial transport appear to differ from each other, and might thus be affected differently during aging (Zala et al., 2013). Thus, it is difficult to extrapolate findings from mitochondrial to vesicular transport or vice versa, and a range of cargoes need to be studied quantitatively to gain a more complete picture of the change in axonal transport during aging. In addition, many studies on age-associated changes in axonal transport analyze only 2 time-points (young and old, or adult and old). This means that the time course of the decline in axonal transport was not well characterized, and the question largely remains as to whether transport decreases slowly throughout adult life, or whether there are periods of sudden change.

Using transgenic animals for live imaging of axonal transport in mice aged 1.5 to 24 months, we observed a pronounced early drop in the rate of NMNAT2-Venus as well as mitochondrial axonal transport in sciatic nerves. In addition, a similar reduction was observed for NMNAT2-Venus particles in optic nerves and the fimbria of the hippocampus. Although the precise timing of this change is tissue dependent, it appears to be complete by 6 months of age in all tissues investigated. These findings are consistent with previous studies in which bulk radiolabeling revealed a reduction in the rate of slow axonal transport between 1 and 6 months of age in peripheral and CNS axons in rats (McQuarrie et al., 1989) and from 2 to 7 months of age in rat sciatic nerves (Tashiro and Komiya, 1994),

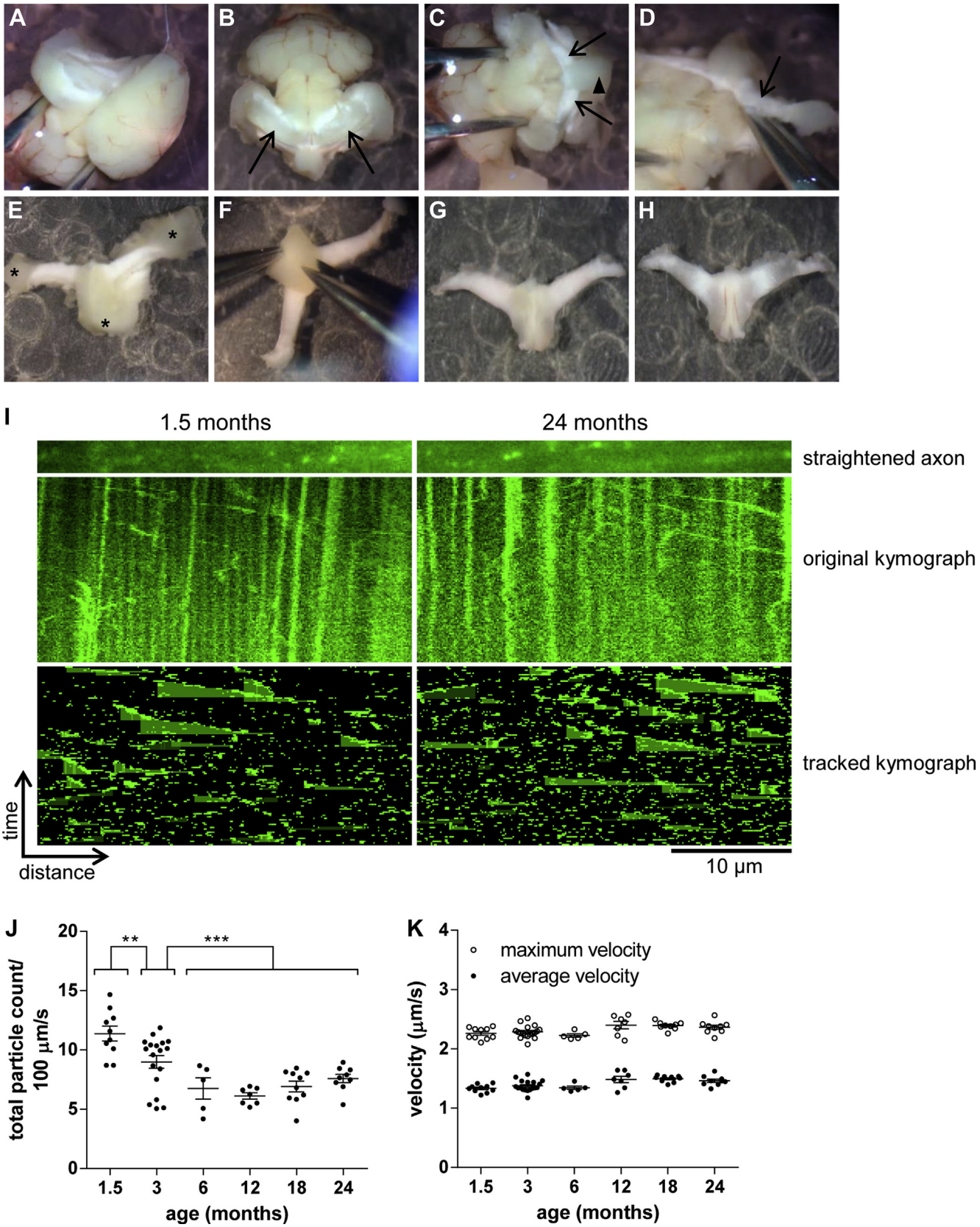

Fig. 4. Age-associated changes in NMNAT2-Venus axonal transport in fimbria. (A-H) Dissection of fimbria for live imaging. (A) Mouse brain in oxygenated Neurobasal A medium with cortex and striatum removed unilaterally. (B) After removal of cortex and striatum on both sides, hippocampi are visible (arrows). (C) Removal of hippocampi exposes the right and left side fimbria (arrows) and the body of fornix (arrowhead). (D) Illustration of dissection to remove the fimbria (right-side fimbria, indicated by arrow) from remainder of the brain. (E) Fimbria and body of fornix after removal from the brain; several pieces of gray matter are still attached and need to be removed before imaging (asterisks). (F) Final step of the clean-up procedure—removal of gray matter (triangular septal nuclei) from the dorsal side of the fornix. (G) Ventral view of the completed explant; this side will be used for live

but the present study reveals how this operates at the level of specific cargoes in individual axons. These early changes could reflect the final stages of growth and development in 1.5- and 3-month-old mice. Even though they are usually considered "young adults," mice at this age are still in the late phase of body growth (Somerville et al., 2004). This means that their peripheral axons are still extending, resulting in a higher demand for energy and cell body-derived structural materials that need to be supplied by axonal transport. At 6 months of age, peripheral axons have reached their final length, and axonal transport has settled to a plateau that is maintained until at least 18 months of age. However, given that skull and brain size do not change significantly after about 1 month of age (Aggarwal et al., 2009; Riquelme et al., 2010), it is difficult to explain the observed drop in axonal transport rates in the optic nerve and fimbria simply through longitudinal axon growth. Other potential late developmental changes that could account for the observed reduction in transport from 1.5 to 3 or 6 months of age include hormonal changes, a decrease in general locomotor and exploratory activity (Elias et al., 1975; Rogers et al., 2001), or late-phase myelination (Agrawal et al., 2009).

The finding that, depending on the precise cargo and tissue, fast axonal transport does not settle down to its "adult plateau" until 3 to 6 months of age also has important implications for the choice of "young" control mice in aging studies more generally. Thus, a comparison of axonal transport rates between 3- and 24-month-old mice would not only detect the old-age drop but also include the much earlier reduction in young adulthood. Our study also demonstrates the importance of the analysis of multiple time-points, as the precise pattern of age-associated changes cannot be deduced from 2 or 3 individual age groups.

Here, we find an early reduction in transport rates of mitochondria in peripheral nerve axons from 3 to 6 months, followed by a stable plateau until at least 12 months of age. Together with results from a previous study in which mitochondrial transport declined significantly from 8 to 24 months of age (Gilley et al., 2012), these results suggest an overall profile for age-associated changes in mitochondrial transport in peripheral axons that is similar to what we found for NMNAT2-Venus, with a significant drop in transport rates between 12 and 24 months. Thus, even though the precise timing of the old-age–associated drop in mitochondrial transport has not been as precisely defined as for NMNAT2, our findings suggest that these 2 cargoes behave in a broadly similar way, indicating that at least some of the underlying mechanisms could be shared as well.

Our results also suggest that changes in fast axonal transport rates are region specific. Interestingly, the reduction in axonal transport of NMNAT2-Venus in 24-month-old animals observed in sciatic and optic nerves was not detectable in fimbria. The fact that the earlier drop between 1.5 and 6 months was readily observed in the fimbria suggests that our method was sensitive enough to detect potential changes. Thus, our data support the conclusion that axonal transport rates in some regions of the aging central nervous system might not change significantly until at least 24 months of age.

For the optic nerve, previous results indicate a reduction in the extent of dendritic and axonal arborization of mouse retinal ganglion cell axons from 3 to 24 months of age (Samuel et al., 2011). However, in the absence of a more detailed time course of the loss of terminal arborization, it is not possible to draw conclusions about any potential causative relationships between the reduction in the rate of NMNAT2-Venus axonal transport and the loss of axonal arbor area. It is, however, interesting to speculate that the extent of an axon's terminal arbor could be 1 of the factors driving age-associated changes. If and when axonal arborization declines with age, axonal transport could fall simply to reflect the reduction in the amount of material needed to support a smaller distal arbor, rather than (or perhaps in addition to) a reduced capacity of the axon to support higher levels of axonal transport. With this in mind, the regeneration experiment may have increased the demand for materials to be delivered to the distal axon to support longitudinal and radial growth, with the axon responding accordingly, rather than necessarily reversing a decline in capacity.

Overall, our results support the conclusion that, at least in peripheral and optic nerves, axonal transport of the axon survival factor NMNAT2 in mice declines substantially at old age, following a previous period of decline at a young adult stage and a relatively stable plateau during adulthood. Given the extensive evidence of impaired axonal transport at early stages in models of neurodegenerative disease (Adalbert and Coleman, 2013; Chevalier-Larsen and Holzbaur, 2006; De Vos et al., 2008), it will be important to extend the study of age-associated changes in axonal transport rates to human aging and age-associated neurodegenerative disease. Albeit technically challenging, this information is vital, given the longer lifespans and more diverse genetic and environmental factors affecting human aging. One method that has been used to study axonal transport rates in humans is the measurement of kinetic biomarkers in cerebrospinal fluid (CSF), which revealed significant impairments in transport rates in Parkinson's disease patients compared to control subjects (Fanara et al., 2012), thus further substantiating findings from animal models that suggest impaired transport rates in neurodegenerative disease. Although no age-associated changes were observed in the control subjects in that study, it is possible that the age span used (36–60 years) corresponds to the "adult plateau" observed in our study, and more extensive investigations using this or similar methods on a broader range of ages are needed to elucidate the time-course of axonal transport changes both in healthy aging humans and in the presence of neurodegenerative disease. It is, for example, interesting to speculate that any disruption of axonal delivery caused by age-associated neurodegenerative disease could synergize with age-associated changes and deplete NMNAT2 levels below its threshold, contributing to axon degeneration in age-associated neurodegeneration.

Importantly, our results also suggest that old neurons in an old systemic environment still have the capacity to sustain higher rates of axonal transport and that appropriate signals can trigger this increase. It will be interesting to determine whether other signals in addition to injury and regeneration can lead to higher rates of axonal transport in old axons. These could include demyelination and remyelination, or the activation of autophagy to promote the clearance of existing axonal structures and the need to deliver new materials into axons. Identifying the signaling pathways, both locally within the axon and within corresponding cell bodies that

imaging. (H) Dorsal view of completed explant. (I) Representative straightened axon, kymograph, and kymograph of tracked particles of NMNAT2-Venus transport in fimbria of 1.5- and 24-month-old NMNAT2-Venus (line 8) mice. The straightened axon represents the first frame of the time lapse recording (total 120 frames; frame rate 2 fps) that was used to generate the original kymograph. Moving particles were tracked using the ImageJ Difference Tracker set of plugins (see Table 2 for parameters) and another kymograph generated to show tracked particles. (J, K) Quantification of axonal transport parameters in fimbria explants from NMNAT2-Venus line 8 animals of indicated ages. Each data point represents the mean value obtained for 1 animal (5 fields of view and, on average, 17 axon tracts per animal). Horizontal bar indicates mean and error bars standard error of the mean. *Indicate statistically significant difference between indicated ages or groups of ages ($^{**}p < 0.01$, $^{***}p < 0.001$; 1-way analysis of variance with Tukey multiple comparisons post-test). The following parameters are shown: (J) total particle count, (K) particle velocity. (For interpretation of the references to color in this Figure, the reader is referred to the web version of this article.)

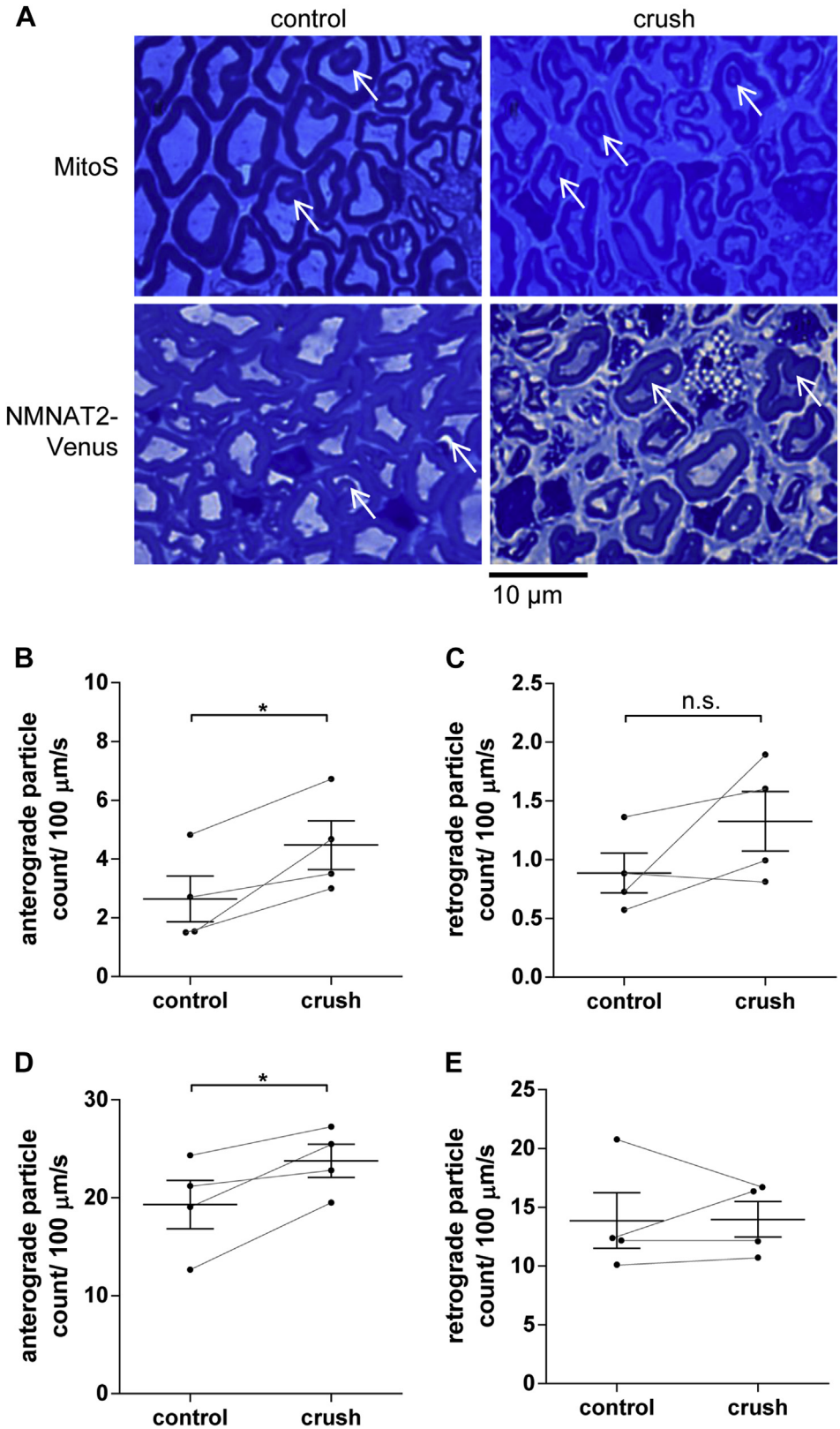

Fig. 5. Partial reversal of age-associated drop in axonal transport of NMNAT2-Venus and mitochondria after nerve crush. (A) Semi-thin sections (500 nm) of control and crushed/regenerated tibial nerves 8 weeks after surgery. White arrows indicate myelin invaginations in all samples. (B, D) Anterograde and (C, E) retrograde particle counts in tibial nerve explants from MitoS (B, C) and NMNAT2-Venus line 8 animals (D, E) at 25 months of age. Eight weeks before imaging, 1 tibial nerve in each animal was crushed (at the level of the distal sciatic nerve) and allowed to regenerate. The contralateral uninjured nerve was used as a control. For all graphs, each data point represents the mean value obtained for 1 animal (6 fields of view and, on average, 15 axons per nerve). Horizontal bar indicates group mean and error bars indicate standard error of the mean. Control and crushed/regenerated nerves from the same animal are connected to indicate matching values. *Statistically significant difference between control and crushed/regenerated nerves (*$p < 0.05$; paired t test). (For interpretation of the references to color in this Figure, the reader is referred to the web version of this article.)

drive the increase in transport capacity, could highlight more targeted means to trigger these changes and to investigate their effects on axon survival during normal aging and in age-associated neurodegenerative disease.

Disclosure statement

The authors declare no competing financial interests.

Acknowledegments

The authors thank Dr Simon Walker for assistance with live imaging. This work was funded by a Medical Research Council (MRC; http://www.mrc.ac.uk) studentship (S.M.), MRC project grant MR/L003813/1 (R.A., S.M.), and a Biotechnology and Biological Sciences Research Council (http://www.bbsrc.ac.uk) Institute Strategic Programme Grant (M.P.C.). The funders had no role in study design, data collection and analysis, decision to publish, or preparation of the manuscript.

References

Adalbert, R., Coleman, M.P., 2013. Axon pathology in age-related neurodegenerative disorders. Neuropathol. Appl. Neurobiol. 39, 90–108.
Adalbert, R., Gillingwater, T.H., Haley, J.E., Bridge, K.E., Beirowski, B., Berek, L., Wagner, D., Grumme, D., Thomson, D., Celik, A., Addicks, K., Ribchester, R.R., Coleman, M.P., 2005. A rat model of slow Wallerian degeneration (WldS) with improved preservation of neuromuscular synapses. Eur. J. Neurosci. 21, 271–277.
Aggarwal, M., Zhang, J., Miller, M.I., Sidman, R.L., Mori, S., 2009. Magnetic resonance imaging and micro-computed tomography combined atlas of developing and adult mouse brains for stereotaxic surgery. Neuroscience 162, 1339–1350.
Agrawal, D., Hawk, R., Avila, R.L., Inouye, H., Kirschner, D.A., 2009. Internodal myelination during development quantitated using x-ray diffraction. J. Struct. Biol. 168, 521–526.
Andrews, S., Gilley, J., Coleman, M.P., 2010. Difference Tracker: ImageJ plugins for fully automated analysis of multiple axonal transport parameters. J. Neurosci. Methods 193, 281–287.
Beirowski, B., Babetto, E., Coleman, M.P., Martin, K.R., 2008. The WldS gene delays axonal but not somatic degeneration in a rat glaucoma model. Eur. J. Neurosci. 28, 1166–1179.
Brunetti, M., Miscena, A., Salviati, A., Gaiti, A., 1987. Effect of aging on the rate of axonal transport of choline-phosphoglycerides. Neurochem. Res. 12, 61–65.
Castel, M., Beaudet, A., Laduron, P., 1994. Retrograde axonal transport of neurotensin in rat nigrostriatal dopaminergic neurons: modulation during ageing and possible physiological role. Biochem. Pharmacol. 47, 53–62.
Chevalier-Larsen, E., Holzbaur, E.L.F., 2006. Axonal transport and neurodegenerative disease. Biochim. Biophys. Acta 1762, 1094–1108.
Chidlow, G., Ebneter, A., Wood, J.P.M., Casson, R.J., 2011. The optic nerve head is the site of axonal transport disruption, axonal cytoskeleton damage and putative axonal regeneration failure in a rat model of glaucoma. Acta Neuropathol. 121, 737–751.
Conforti, L., Gilley, J., Coleman, M.P., 2014. Wallerian degeneration: an emerging axon death pathway linking injury and disease. Nat. Rev. Neurosci. 15, 394–409.
Cross, D.J., Flexman, J.A., Anzai, Y., Maravilla, K.R., Minoshima, S., 2008. Age-related decrease in axonal transport measured by MR imaging in vivo. Neuroimage 39, 915–926.
De Vos, K.J., Grierson, A.J., Ackerley, S., Miller, C.C.J., 2008. Role of axonal transport in neurodegenerative diseases. Annu. Rev. Neurosci. 31, 151–173.
Elias, P.K., Elias, M.F., Eleftheriou, B.E., 1975. Emotionality, exploratory behavior, and locomotion in aging inbred strains of mice. Gerontologia 21, 46–55.
Fanara, P., Wong, P.A., Husted, K.H., Liu, S., Liu, V.M., Kohlstaedt, L.A., Riiff, T., Protasio, J.C., Boban, D., Killion, S., Killian, M., Epling, L., Sinclair, E., Peterson, J., Price, R.W., Cabin, D.E., Nussbaum, R.L., Brühmann, J., Brandt, R., Christine, C.W., Aminoff, M.J., Hellerstein, M.K., 2012. Cerebrospinal fluid-based kinetic biomarkers of axonal transport in monitoring neurodegeneration. J. Clin. Invest. 122, 3159–3169.
Fernandez, H.L., Hodges-Savola, C.A., 1994. Axoplasmic transport of calcitonin gene-related peptide in rat peripheral nerve as a function of age. Neurochem. Res. 19, 1369–1377.
Frolkis, V.V., Tanin, S.A., Gorban, Y.N., 1997. Age-related changes in axonal transport. Exp. Gerontol. 32, 441–450.
Geinisman, Y., Bondareff, W., Telser, A., 1977. Diminished axonal transport of glycoproteins in the senescent rat brain. Mech. Ageing 6, 363–378.
Gilley, J., Adalbert, R., Yu, G., Coleman, M.P., 2013. Rescue of peripheral and CNS axon defects in mice lacking NMNAT2. J. Neurosci. 33, 13410–13424.
Gilley, J., Coleman, M.P., 2010. Endogenous Nmnat2 is an essential survival factor for maintenance of healthy axons. PLoS Biol. 8, e1000300.
Gilley, J., Seereeram, A., Ando, K., Mosely, S., Andrews, S., Kerschensteiner, M., Misgeld, T., Brion, J.P., Anderton, B., Hanger, D.P., Coleman, M.P., 2012. Age-dependent axonal transport and locomotor changes and tau hyperphosphorylation in a "P301L" tau knockin mouse. Neurobiol. Aging 33, 621.e1–621.e15.
Goemaere-Vanneste, J., Couraud, J.Y., Hassig, R., Di Giamberardino, L., van den Bosch de Aguilar, P., 1988. Reduced axonal transport of the G4 molecular form of acetylcholinesterase in the rat sciatic nerve during aging. J. Neurochem. 51, 1746–1754.
Hirokawa, N., Noda, Y., 2008. Intracellular transport and kinesin superfamily proteins, KIFs: structure, function, and dynamics. Physiol. Rev. 88, 1089.
Hirokawa, N., Noda, Y., Tanaka, Y., Niwa, S., 2009. Kinesin superfamily motor proteins and intracellular transport. Nat. Rev. Mol. Cell Biol. 10, 682–696.
Howell, G.R., Libby, R.T., Jakobs, T.C., Smith, R.S., Phalan, F.C., Barter, J.W., Barbay, J.M., Marchant, J.K., Mahesh, N., Porciatti, V., Whitmore, A.V., Masland, R.H., John, S.W.M., 2007. Axons of retinal ganglion cells are insulted in the optic nerve early in DBA/2J glaucoma. J. Cell Biol. 179, 1523–1537.
Lau, C., Dölle, C., Gossmann, T.I., Agledal, L., Niere, M., Ziegler, M., 2010. Isoform-specific targeting and interaction domains in human nicotinamide mononucleotide adenylyltransferases. J. Biol. Chem. 285, 18868–18876.
Li, W., Hoffman, P.N., Stirling, W., Price, D.L., Lee, M.K., 2003. Axonal transport of human α-synuclein slows with aging but is not affected by familial Parkinson's disease-linked mutations. J. Neurochem. 88, 401–410.
Mar, F.M., Simões, A.R., Leite, S., Morgado, M.M., Santos, T.E., Rodrigo, I.S., Teixeira, C.A., Misgeld, T., Sousa, M.M., 2014. CNS axons globally increase axonal transport after peripheral conditioning. J. Neurosci. 34, 5965–5970.
Marinkovic, P., Reuter, M.S., Brill, M.S., Godinho, L., Kerschensteiner, M., Misgeld, T., 2012. Axonal transport deficits and degeneration can evolve independently in mouse models of amyotrophic lateral sclerosis. Proc. Natl. Acad. Sci. U. S. A. 109, 4296–4301.
McMartin, D., O'Conner, J.J., 1979. Effect of age on axoplasmic transport of cholinesterase in rat sciatic nerves. Mech. Ageing Dev. 10, 241–248.
McQuarrie, I.G., Brady, S.T., Lasek, R.J., 1989. Retardation in the slow axonal transport of cytoskeletal elements during maturation and aging. Neurobiol. Aging 10, 359–365.
Milde, S., Fox, A.N., Freeman, M.R., Coleman, M.P., 2013a. Deletions within its subcellular targeting domain enhance the axon protective capacity of Nmnat2 in vivo. Sci. Rep. 3, 2567.
Milde, S., Gilley, J., Coleman, M.P., 2013b. Subcellular localization determines the stability and axon protective capacity of axon survival factor Nmnat2. PLoS Biol. 11, e1001539.
Millecamps, S., Julien, J.P., 2013. Axonal transport deficits and neurodegenerative diseases. Nat. Rev. Neurosci. 14, 161–176.
Misgeld, T., Kerschensteiner, M., Bareyre, F.M., Burgess, R.W., Lichtman, J.W., 2007. Imaging axonal transport of mitochondria in vivo. Nat. Methods 4, 559–561.
Riquelme, R., Cediel, R., Contreras, J., la Rosa Lourdes, R., Murillo-Cuesta, S., Hernandez-Sanchez, C., Zubeldia, J.M., Cerdan, S., Varela-Nieto, I., 2010. A comparative study of age-related hearing loss in wild type and insulin-like growth factor I deficient mice. Front. Neuroanat. 4, 27.
Rogers, D.C., Peters, J., Martin, J.E., Ball, S., Nicholson, S.J., Witherden, A.S., Hafezparast, M., Latcham, J., Robinson, T.L., Quilter, C.A., Fisher, E.M., 2001. SHIRPA, a protocol for behavioral assessment: validation for longitudinal study of neurological dysfunction in mice. Neurosci. Lett. 306, 89–92.
Samuel, M.A., Zhang, Y., Meister, M., Sanes, J.R., 2011. Age-related alterations in neurons of the mouse retina. J. Neurosci. 31, 16033–16044.
Somerville, J.M., Aspden, R.M., Armour, K.E., Armour, K.J., Reid, D.M., 2004. Growth of C57BL/6 mice and the material and mechanical properties of cortical bone from the tibia. Calcif. Tissue Int. 74, 469–475.
Stromska, D.P., Ochs, S., 1982. Axoplasmic transport in aged rats. Exp. Neurol. 77, 215–224.
Tanaka, K., Webster, H.D., 1991. Myelinated fiber regeneration after crush injury is retarded in sciatic nerves of aging mice. J. Comp. Neurol. 308, 180–187.
Tanaka, K., Zhang, Q.L., Webster, H.D., 1992. Myelinated fiber regeneration after sciatic nerve crush: morphometric observations in young adult and aging mice and the effects of macrophage suppression and conditioning lesions. Exp. Neurol. 118, 53–61.
Tashiro, T., Komiya, Y., 1994. Impairment of cytoskeletal protein transport due to aging or beta,beta′-iminodipropionitrile intoxication in the rat sciatic nerve. Gerontology 40 (Suppl 2), 36–45.
Viancour, T.A., Kreiter, N.A., 1993. Vesicular fast axonal transport rates in young and old rat axons. Brain Res. 628, 209–217.
Wang, X., Schwarz, T.L., 2009. The mechanism of Ca2+-dependent regulation of kinesin-mediated mitochondrial motility. Cell 136, 163–174.
Zala, D., Hinckelmann, M.V., Yu, H., Lyra da Cunha, M.M., Liot, G., Cordelières, F.P., Marco, S., Saudou, F., 2013. Vesicular glycolysis provides on-board energy for fast axonal transport. Cell 152, 479–491.